JOURNAL OF GEOPHYSICAL RESEARCH, VOL. 103, NO. C2, PAGES 3249–3255, FEBRUARY 15, 1998

An inertial-dissipation method for estimating turbulent flux in buoyancy-driven, convective boundary layers

Miles G. McPhee
McPhee Research Company, Naches, Washington

Abstract. A method is developed for using wavenumber spectra of scalar contaminants in a boundary layer dominated by buoyancy-driven convection to estimate the magnitude of vertical turbulent fluxes. The technique is analogous to the conventional inertial-dissipation method (IDM) for obtaining fluxes from variance spectral density levels in the inertial subrange but differs in the way that turbulence scales are combined to provide an "eddy density diffusivity" for relating flux magnitude to variance dissipation rate. The method is illustrated using spectra and direct flux covariance data from the oceanic boundary layer at the edge of a freezing lead during the 1992 Lead Experiment in the Arctic Ocean. There, density was controlled almost exclusively by salinity, and it is argued that the turbulent length and velocity scales governing vertical exchange were the inverse of the wavenumber at the peak in the weighted salinity spectrum (considerably less than the mixed layer depth) and the cube root of the product of turbulent length scale and the buoyancy flux magnitude, respectively. The sign of the skewness of temperature or salinity time series is shown to be a robust indicator of the (negative) direction of vertical flux. The "free convection" approach is valid (i.e., should be used instead of the conventional IDM) only if the convective turbulent scale velocity is appreciably larger than friction velocity (square root of the Reynolds stress), so that turbulent kinetic energy dissipation is approximately equal to buoyancy production.

1. Background

The magnitude of Reynolds stress (momentum flux) in a shear-driven turbulent flow may be estimated by calculating the dissipation rate, ε, of turbulent kinetic energy (TKE) from power spectral density levels in the inertial subrange and by equating ε to the production of TKE by shear, which is the dot product of Reynolds stress and mean shear [e.g., *Hinze*, 1975]. The technique may be extended to estimate the flux of a scalar contaminant (such as salinity) by calculating the variance dissipation rate (e.g., ε_S) from spectral density in the inertial subrange of the variance spectrum of the contaminant and by equating it with the "production of variance" (the product of the flux and mean gradient). Called the "inertial-dissipation method" (IDM), the technique has been applied widely for estimating Reynolds stress and turbulent heat and moisture fluxes in the atmospheric surface layer [e.g., *Edson et al.*, 1991] and occasionally for estimating stress near the seafloor in the benthic boundary layer [*Gross and Nowell*, 1985].

A strong incentive exists for developing a practical IDM for estimating turbulent fluxes in boundary layers of the ocean because it is generally much easier to measure wavenumber spectra to scales in the inertial subrange (typically of order 1 m) than it is to measure zero-lag covariances (e.g., $\langle w'S' \rangle$, where w' and S' are the deviatory vertical velocity and salinity, respectively), especially if platform motion is present. Microstructure profiling techniques, which measure in the dissipation range of the turbulent spectrum, may also be used to estimate variance dissipation but suffer from difficulty in distinguishing between salinity (measured via conductivity) and temperature variability at high frequencies (small scales).

It is often difficult to reliably measure vertical shear and scalar gradients in the so-called mixed layer that nearly always exists above the pycnocline in the ocean; thus one thrust of my recent research has been developing methods for estimating eddy viscosity, or mixing length, from point measurements in order to extract shear production of TKE, i.e.,

$$\tau \frac{\partial U}{\partial z} = \frac{u_*^4}{K} = \frac{u_*^3}{\lambda}, \tag{1}$$

where τ is kinematic turbulent stress, U is mean horizontal velocity, $u_* = \sqrt{\tau}$ is the friction velocity, K is eddy viscosity, and $\lambda = K/u_*$ is the mixing length. Recent work [*McPhee and Martinson*, 1994; *McPhee*, 1994; *McPhee and Stanton*, 1996, hereinafter referred to as MS] has demonstrated that λ is inversely proportional to the wavenumber at the peak in the weighted (slope) variance spectrum of vertical velocity and confirmed that the inertial-dissipation technique provides a viable means of estimating flux magnitudes from point measurements in the oceanic boundary layer under drifting pack ice.

My approach to IDM [*McPhee*, 1994] depends on friction velocity and thus tacitly assumes that the scale velocity is determined by surface stress. As with other boundary layer techniques based on u_*, problems are encountered as shear-driven stress decreases, and convection from destabilizing surface buoyancy flux becomes the dominant source of turbulence. In highly convective regimes where mean vertical shear is small, dimensional reasoning suggests that the proper turbulent scaling velocity, w_*, depends on the surface buoyancy flux, $\langle w'b' \rangle_0 = (g/\rho)\langle w'\rho' \rangle_0$ (where g is the acceleration of gravity, w is vertical velocity, ρ is fluid density, and primes indicate devia-

Copyright 1998 by the American Geophysical Union.

Paper number 97JC02263.
0148-0227/98/97JC-02263$09.00

tion from the mean value), and a dominant turbulent length scale, λ, i.e.,

$$w_* = (\lambda|\langle w'b'\rangle|_0)^{1/3}. \quad (2)$$

In "free convection" planetary boundary layer problems the length scale is often taken to be $\lambda = D$, where D is the vertical extent of the well mixed layer, or equivalently, the distance to the pycnocline, hence $W_* = (D|\langle w'b'\rangle|)^{1/3}$ [e.g., *Shay and Gregg*, 1986].

The 1992 Lead Experiment (LeadEx) offered a rare opportunity to observe turbulence in the oceanic boundary layer under statically unstable surface flux conditions induced by salt rejection during rapid freezing [*LeadEx Group*, 1993; MS; *Morison and McPhee*, this issue]. We were able to airlift a temporary ice camp into position and make a full suite of upper ocean turbulence measurements at the "downstream" (upwind) edges of two rapidly freezing leads (leads 3 and 4). Salt-driven convection differed at the two sites [*Morison and McPhee*, this issue]. At lead 3 a persistent breeze moved the ice pack (and its embedded lead, which was about a kilometer wide) downwind at around 12–13 cm s^{-1} relative to the underlying ocean. This led to a forced convective regime [e.g., *Morison et al.*, 1992], where both shear and buoyancy were important in the production of TKE through most of the boundary layer and in which most of the turbulent transport occurred in large, quasi-organized convective features advected past our instruments with the mean flow (MS). At lead 4, which was about 100 m wide, current measured from the drifting ice was one quarter to one third as large as at lead 3. Turbulence at the downstream edge of lead 4 was dominated by buoyancy flux. Horizontal transects made by an autonomous underwater vehicle perpendicular to the lead indicated that the major convective cells clustered near the lead edges [*Morison and McPhee*, this issue]. Thus lead 4 approached a state of free convection, where wind-driven shear played a secondary role.

Time series of turbulence data were obtained at four levels spanning 6 m at the downstream edges of both leads, from a mast equipped with turbulence instrument clusters (TICs). Each TIC measures the three-dimensional flow plus temperature and conductivity. Performance of the system, including one cluster equipped with a microstructure conductivity sensor capable of measuring the salinity variance spectrum well into the inertial subrange, is described by MS. The current meter device comprises three small rotors arranged in an orthogonal triad, with one component (v_m) horizontal and the others canted 45° down (u_m) and up (w_m) from horizontal, respectively. By a simple coordinate transformation (in practice, a rotation into a streamline coordinate system) this furnishes a continuous record of vertical velocity, provided the mean flow is sufficient to keep all three rotors turning above their individual stall thresholds, typically between 1 and 2 cm s^{-1}. Measuring the total velocity vector is thus problematic when the mean flow velocity is small, as at lead 4. By good fortune the one cluster (TIC number 2) for which both u_m and w_m (the components necessary for determining vertical velocity) turned consistently was also equipped with the microstructure conductivity sensor, so that the scalar flux covariances ($\langle w'T'\rangle$ and $\langle w'S'\rangle$, where T' is the deviatory temperature) could be estimated (MS). A search of velocity records from TIC 2 yielded 16 independent 1-hour segments when both w_m and u_m components turned for at least 70% of the time. It was not possible to calculate the Reynolds stress tensor for TIC 2 because its v_m (horizontal) rotor did not turn consistently; however, the mean v_m flow component could be closely estimated by using the rotor from TIC 3 (2 m lower), which did turn.

Despite these shortcomings in velocity measurements, data from lead 4 provided wavenumber variance spectra for temperature and salinity, along with viable estimates of the Reynolds fluxes for heat and salt in a flow regime approaching free convection. These are the essential elements for testing a method for estimating fluxes from the spectra. The purpose of the present work is to suggest an extension of the inertial-dissipation method appropriate for free convection conditions encountered at lead 4. In the next section the technique is developed by analogy with the shear-driven case [*McPhee*, 1994] and illustrated by LeadEx data. Results, including a comparison with data from the forced convective regime at lead 3 and a means of determining flux direction, are discussed and summarized in section 3.

2. Inertial-Dissipation Technique in Turbulence Dominated by Convection

If an inertial subrange exists in a turbulent flow, there is a simple relation between spectral levels at wavenumbers within the inertial subrange and the dissipation rate, ε, of turbulent kinetic energy [e.g., *Hinze*, 1975],

$$\varepsilon^{2/3} = \frac{3}{4\alpha_\varepsilon} S_{ww}(k)k^{5/3}, \quad (3)$$

where $S_{ww}(k)$ is the spectral energy density ($m^3\ s^{-2}$) for the vertical velocity component at angular wavenumber, k (rad m^{-1}), and α_S is the Kolmogorov constant, with numerical value found from atmospheric and laboratory studies to be about 0.51. For scalar variables in a fully developed turbulent flow a similar relationship holds between the scalar variance dissipation and variance spectral levels in the inertial subrange, e.g., for salinity,

$$\varepsilon_S = \frac{\varepsilon^{1/3}}{\alpha_S} S_{SS}(k)k^{5/3}, \quad (4)$$

where ε_S is the salinity variance dissipation rate, $S_{SS}(k)$ is the salinity variance spectral density, and α_S is the Kolmogorov constant for scalar salinity. *McPhee and Stanton* [1996] verified that α_S was of order unity, using direct $\langle w'S'\rangle$ covariance and spectral measurements from the forced convection regime at lead 3.

By analogy with the TKE equation the salinity flux is estimated from the salinity variance dissipation by assuming that the production of variance by interaction between the flux and the mean gradient is equal to the dissipation,

$$-\langle w'S'\rangle \frac{\partial S}{\partial z} = \varepsilon_S. \quad (5)$$

The obvious problem in calculating salinity flux by applying (5) is obtaining the mean gradient (which is very small in the mixed layer) at the point where the spectrum is measured. However, if the eddy diffusivity for salinity, K_S, is known, (5) yields a formula for the flux magnitude, $|\langle w'S'\rangle| = \sqrt{K_S\varepsilon_S}$.

For the neutrally stratified, stress-driven turbulent boundary layer under drifting ice, we found [*McPhee and Martinson*, 1994] that the mean shear at a specific level could be well estimated by relating the shear to stress using an eddy viscosity, $K = u_*\lambda$, as in (1). In a low-stress, convective regime driven

by surface freezing it seems unlikely that an approach based on friction velocity would be appropriate; however, it does suggest a testable hypothesis using an analogous scheme. Since buoyancy flux controls the turbulence, the eddy diffusivity for mass flux is postulated to be $K_\rho = w_* \lambda_\rho$, where λ_ρ is the dominant turbulent scale in the buoyancy-driven flow and w_* is given by (2) with $\lambda = \lambda_\rho$. Furthermore, at temperatures near freezing the coefficient of thermal expansion is very small, so buoyancy flux depends almost exclusively on salinity flux,

$$\langle w'b' \rangle = g\beta_S \langle w'S' \rangle, \tag{6}$$

where β_S is the saline contraction coefficient, yielding an equation for the magnitude of salinity flux in terms of salinity variance dissipation and a length scale characterizing the turbulence,

$$\frac{|\langle w'S' \rangle|^2}{K_S} = \frac{|\langle w'S' \rangle|^{5/3}}{\lambda_S^{4/3}(\beta_S g)^{1/3}} = \varepsilon_S. \tag{7}$$

In the lead studies, buoyancy depends on salinity (temperature is essentially a passive tracer), so we assume that λ_ρ is inversely proportional to the wavenumber at the peak of the weighted salinity spectrum. Thus (7) constitutes a direct analog to the conventional inertial-dissipation method for estimating turbulent stress from TKE dissipation in the neutrally stable boundary layer where turbulence is controlled by the flux of momentum, i.e., $u_*^3 = \varepsilon\lambda$ [*McPhee*, 1994].

The "free convection IDM" is illustrated using averages of spectra calculated for each of eight, 1-hour segments of data from TIC 2 (equipped with a microstructure conductivity meter) at lead 4. Only segments for which the downward covariance salinity flux exceeded 5×10^{-6} psu m s^{-1}, representing the most intense convective conditions, were included. Weighted vertical velocity and salinity spectra are plotted in logarithmic coordinates in Figure 1, where the solid curve is a high-order polynomial fitted to the binned spectral estimates. After some experimentation a standardized method of picking a weighted spectral density ordinate indicative of the inertial subrange was chosen using the first abscissa past the spectral peak for which the magnitude of the slope equaled or exceeded two thirds. These are indicated in Figure 1 by the horizontal dashed lines, which were used in (3) and (4) to calculate TKE and salinity variance dissipation rates, yielding $\varepsilon = 4.0 \times 10^{-8}$ W kg^{-1} and $\varepsilon_S = 2.5 \times 10^{-9}$ psu^2 s^{-1}. The length scale is inversely proportional to the wavenumber at the peak in the weighted S spectrum as indicated by the vertical line in Figure 1b, $\lambda = 1/k_{\max} = 3.0$ m. From (7), the spectral estimate of salinity flux magnitude is $|\langle w'S' \rangle|_{\text{Spec1}} = 6.3 \times 10^{-6}$ psu m s^{-1}, nearly the same as the average direct zero-lag covariance: $|\langle w'S' \rangle| = 6.3 \times 10^{-6}$ psu m s^{-1}. The turbulent scaling velocity, $w_* = (|\langle w'b' \rangle| \lambda_S)^{1/3}$, is 0.52 cm s^{-1}, which is less than half the convective velocity W_* based on buoyancy flux and mixed layer depth: 1.1 cm s^{-1} (mixed layer depth was 28 m based on visual inspection of the salinity profiles).

For practical application the inertial-dissipation method usually assumes a balance among three major terms in the TKE equation: production by shear, production by buoyancy, and dissipation. In free convection the turbulent kinetic energy production by shear is negligible compared with buoyancy production, so that the steady state, horizontally homogeneous TKE equation reduces to

$$-\langle w'b' \rangle = \varepsilon. \tag{8}$$

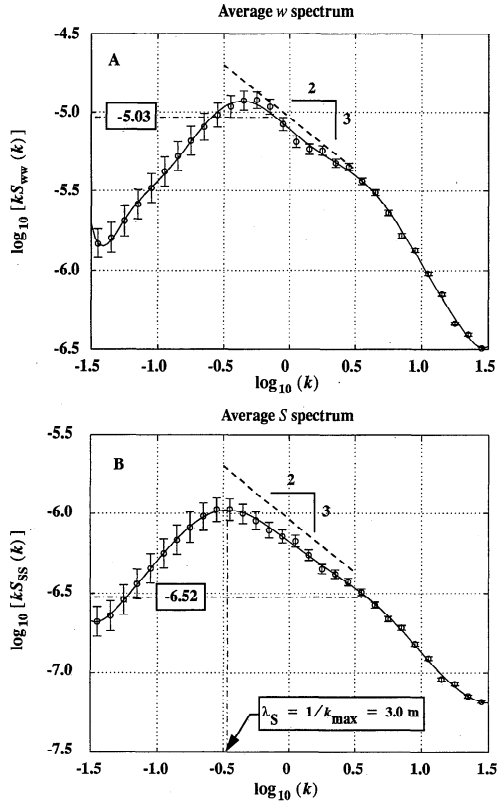

Figure 1. Weighted (spectral density multiplied by wavenumber) variance spectra for (a) vertical velocity and (b) salinity averaged from eight 1-hour time series during the LeadEx lead 4 deployment. For each segment, covariance salinity flux exceeded 5×10^{-6} psu m s^{-1}. Depth of the instrument cluster was 3.3 m in a 28-m-deep mixed layer. Error bars indicate the 95% confidence interval for spectral estimates averaged in 30 equal bins of the logarithmic wavenumber (rad m^{-1}) axis. Curves are high-order polynomial fit. Horizontal lines show the spectral levels used to estimate ε and ε_S.

To the degree that the assumptions leading to (7) and (8) are valid, salinity flux may be estimated solely from the salinity variance spectrum by combining (4), (7), and (8). Using only the salinity spectrum of Figure 1b, the estimated salinity flux was $|\langle w'S' \rangle|_{\text{Spec2}} = 6.7 \times 10^{-6}$ psu m s^{-1}, about 6% greater than the other estimates. The corresponding buoyancy production (4.8×10^{-8} W kg^{-1}) was about 20% greater than dissipation ($\varepsilon = 4.0 \times 10^{-8}$ W kg^{-1}) estimated from the w spectrum. The latter is subject to uncertainties in w due to rotor stalls as discussed below.

Individual spectra of 1-hour time series show considerably more scatter than the averaged spectra; however, if an underlying inertial subrange is assumed and the spectral estimates fitted with a polynomial, the spectral characteristics of each 1-hour segment may be estimated and used to construct a time series of salinity flux estimates for comparison with covariance measurement (Figure 2). The shaded envelope indicates a range of covariance values corresponding to differing treatment of vertical velocity. For the low end of the range, only velocity samples for which both u_m and w_m were both turning (nonzero) were used to calculate covariance. This is thought to underestimate the flux because one of the current meter rotors often stalled when the pitch (angle of attack relative to horizontal) was greatest, i.e., times when $|w|$ was large. The high-

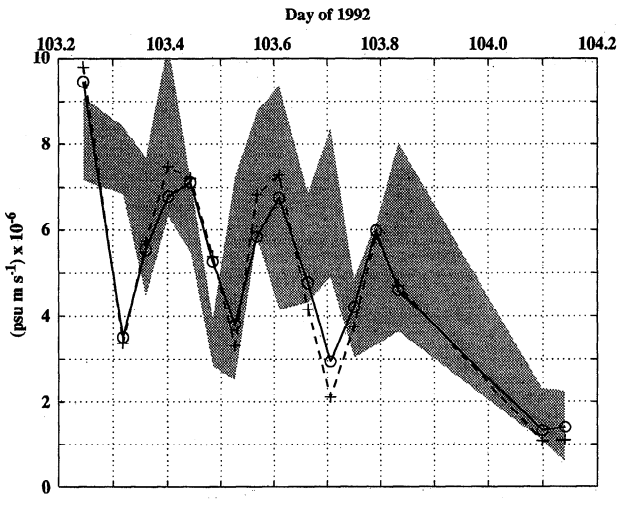

Figure 2. Lead 4 estimates of salinity flux from 1-hour time series of vertical velocity and linearly detrended salinity. The shaded curve shows the range of direct zero-lag covariance, $|\langle w'S'\rangle|$, calculated under two assumptions for vertical velocity as discussed in the text. The solid curve with open circles is from (7) with ε_S and λ_S from the salinity variance spectrum using ε obtained from the vertical velocity power spectrum ($|\langle w'S'\rangle|_{\text{Spec1}}$). The dashed curve with crosses is from (7) solved entirely from the salinity spectrum, with ε obtained from the buoyancy flux ($|\langle w'S'\rangle|_{\text{Spec2}}$).

magnitude side of the envelope corresponds to covariance calculated from the entire time series, including zeros. This probably overestimates flux magnitude because it introduces spurious variance as a particular rotor goes suddenly to zero when the current passing through it falls below stall threshold. Mean values for the low- and high-covariance estimates are 4.1×10^{-6} and 7.0×10^{-6} psu m s^{-1}, respectively. The actual mean value is probably between these limits, and a conservative but more realistic estimate is one in which the vertical component is calculated from nonzero values of u_m and w_m and then interpolated linearly in the gaps. The average value using linearly interpolated w is $|\langle w'S'\rangle| = 4.7 \times 10^{-6}$ psu m s^{-1}. Inertial-subrange (spectral) estimates of flux magnitude were made by both methods described above, from S and w spectra (open circles, with mean value $|\langle w'S'\rangle|_{\text{Spec1}} = 5.0 \times 10^{-6}$ psu m s^{-1}) and from the salinity spectrum alone (crosses, mean value $|\langle w'S'\rangle|_{\text{Spec2}} = 4.9 \times 10^{-6}$ psu m s^{-1}). The two methods agree well with each other and generally follow the covariance envelope. Regression of salinity flux estimates against measured $\langle w'S'\rangle$ covariance (from linearly interpolated w) is illustrated in Figure 3. While the confidence limits on the regressions slopes are large, the result justifies the choice of parameters in the inertial-subrange approach, namely, $\alpha_S = 1$ and $\lambda_S = 1/k_{\max}$.

Further confirmation of the basic scaling is provided in Figure 4 by a comparison between heat flux magnitude estimated from $\langle w'T'\rangle$ covariances and flux magnitude obtained from the temperature variance spectra. The shaded envelope reflects the same treatment of vertical velocity as for salinity flux. Temperature variance dissipation was obtained from the thermal counterpart of (4),

$$\varepsilon_T = \frac{\varepsilon^{1/3}}{\alpha_T} S_{TT}(k) k^{5/3}, \tag{9}$$

with $\alpha_T = 0.85$ (MS), and $\varepsilon = g\beta_S|\langle w'S'\rangle|_{\text{Spec2}}$, i.e., buoyancy production estimated solely from the wavenumber spectrum of salinity variance. Heat flux magnitude follows from the analog of (5),

$$\langle w'T'\rangle \frac{\partial T}{\partial z} = \frac{|\langle w'T'\rangle|^2}{w_* \lambda_\rho} = \varepsilon_T, \tag{10}$$

where again w_* and λ_ρ are obtained from the salinity spectrum, assuming that eddy diffusivities for heat and salt are similar (Reynolds analogy). Over the 16 hourly samples, using

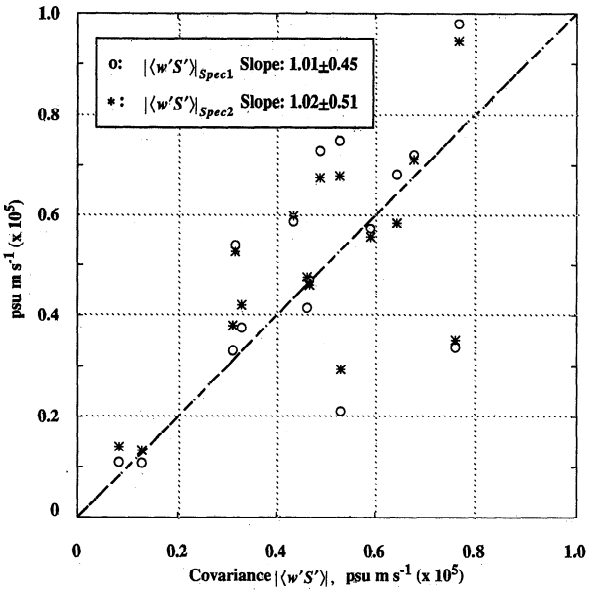

Figure 3. Regression of salinity flux calculated using w and S spectra ($|\langle w'S'\rangle|_{\text{Spec1}}$) and calculated from the S spectrum alone ($|\langle w'S'\rangle|_{\text{Spec2}}$) against the covariance flux magnitude. Regression slopes with 95% confidence intervals are indicated in the legend.

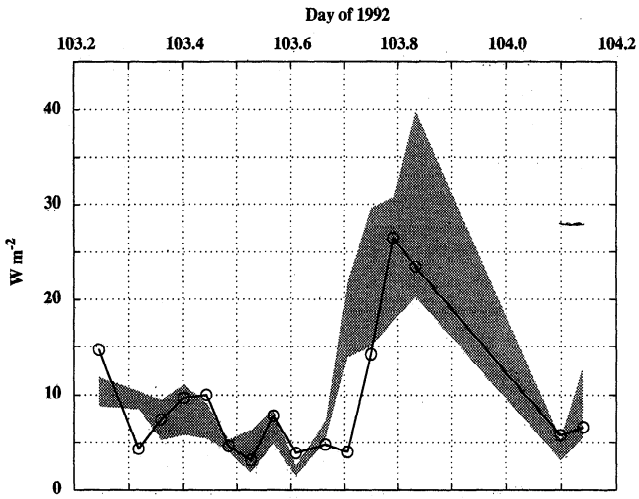

Figure 4. Estimates of turbulent heat flux magnitude at lead 4. The shaded area shows the range of covariance estimates using differing w treatments as in Figure 2. The solid curve with open circles shows an estimate based on temperature variance spectrum, with turbulent kinetic energy (TKE) dissipation and eddy diffusivity obtained from the salinity spectrum.

w interpolated in gaps due to rotor stall, the average value of covariance heat flux magnitude is $\rho c_p|\langle w'T'\rangle| = 9.2$ W m^{-2}. For the inertial-subrange estimate from the T and S spectra the mean value is 9.4 W m^{-2}. Note that the spectral method does not indicate flux direction. At both leads 3 and 4, salinity flux was always downward, while heat flux was upward at night and downward during daylight hours (MS).

3. Discussion

The purpose of this note is to propose a means of estimating the vertical flux of a scalar quantity in a convective boundary layer from wavenumber spectra alone, i.e., without knowledge of the covariance of the quantity with vertical velocity or of its mean gradient in the "mixed layer." The method depends on four properties, all derived from the spectra: the turbulent scale velocity (w_* or u_*), vertical turbulent exchange length scale (λ), the TKE dissipation rate (ε), and the dissipation rate for scalar variance of the property that controls density (in this case, ε_S). It rests on the assumption that the dominant length scale is inversely proportional to the wavenumber at the peak in the weighted (slope) spectrum of the scalar controlling density. This is not well established but derives from analogy with work relating the peak in the weighted w spectrum to the dominant length scale in shear driven flows [*McPhee*, 1994]. The essential idea is that the peak in the weighted spectrum indicates a scale associated with the most energetic turbulent eddies (it is a vertical exchange scale, not "wavelength" associated with the peak, which is $2\pi/k_{max}$).

If the vertical velocity spectrum is known, it provides ε. When mean horizontal current is small or when sampling with autonomous underwater vehicles, it is often much easier to measure spectra of scalar properties. An alternative method, which depends only on the spectrum of the scalar controlling buoyancy (normally temperature or salinity), estimates ε by equating it to buoyancy production. This approximation is generally accepted for flows where u_* is small. Hence, if buoyancy flux is the main source of turbulence, the eddy diffusivity is

$$K_\rho = w_*\lambda_\rho = \lambda_\rho^{4/3}|\langle w'b'\rangle|^{1/3}, \tag{11}$$

whereas if shear is the dominant source, the scale from the w spectrum, λ_w, governs, the eddy viscosity is $K = u_*\lambda_w$, and eddy diffusivity follows.

What about forced convection, where both shear and buoyancy feed the turbulence? At lead 3 the drift velocity (essentially the shear between the ice and mixed layer) was 3 to 4 times larger than at lead 4. The ratio of mixed layer depth to Obukhov length (taken as a measure of the relative strength of buoyancy to shear forcing) was comparatively small (~ -2), and it appeared that the turbulence regime was essentially shear driven, with turbulence significantly enhanced by destabilizing surface buoyancy flux (MS). Data from lead 3 (forced convection) were analyzed in order to compare the free convection IDM with the more conventional method based on shear-driven estimates of eddy viscosity. Nine 1-hour segments of data from the microconductivity-equipped TIC, when it was positioned at 4.3 m depth (similar to the lead 4 deployment), were considered. In Figure 5, three evaluations of $|\langle w'S'\rangle|$ are shown. The shaded curve indicates ranges for directly measured covariances with the treatment of dropouts in w as before. The mean covariance estimate of salinity flux for the nine segments is $|\langle w'S'\rangle| = 0.96 \times 10^{-5}$ psu m s^{-1}. The curve

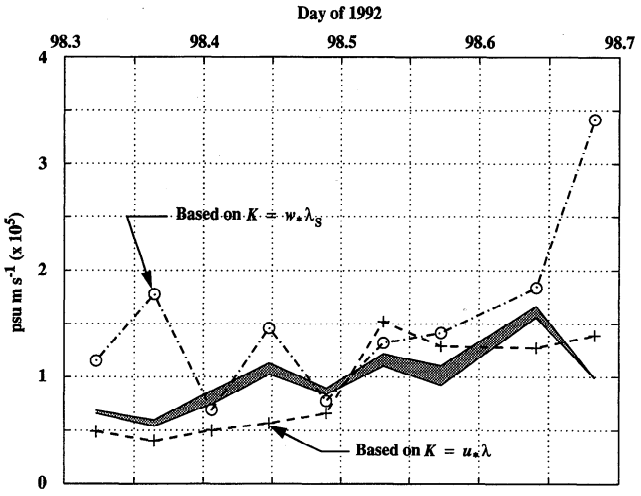

Figure 5. Estimates of turbulent salinity flux magnitude at lead 3 (forced convection). The shaded area shows the range of covariance estimates using differing w treatments as in Figure 2. The dot-dashed curve with open circles shows an inertial-dissipation estimate based on salinity spectrum alone ($|\langle w'S'\rangle|_{Spec2}$). The dashed curve with crosses shows an inertial-dissipation estimate with $K = u_*\lambda$, where u_* is the square root of the measured kinematic turbulent stress and λ is the mixing length from the w spectrum.

marked with open circles is the free convection IDM estimate from the salinity spectrum only. Its mean value is $|\langle w'S'\rangle|_{Spec2} = 1.54 \times 10^{-5}$ psu m s^{-1}. The third curve is the IDM estimate using the same value for ε_S (obtained from the inertial subrange of the S spectrum) but with a different eddy viscosity based on the measured friction velocity (u_*) and λ_w from the w spectrum (MS), so that

$$|\langle w'S'\rangle|_{u_*} = (u_*\lambda_w\varepsilon_S)^{1/2}. \tag{12}$$

The mean value is $\overline{|\langle w'S'\rangle|_{u^*}} = 0.90 \times 10^{-5}$ psu m s^{-1}. Thus eddy viscosity based on the stress-driven aspects of the flow may have been more appropriate at lead 3. It should be noted, however, that λ_w was much larger than would be expected for neutral stratification because of the effect of destabilizing buoyancy flux [see *McPhee*, 1994, Figures 11 and 14].

A shortcoming of the IDM is that it does not by itself furnish the sign (direction) of vertical flux. However, another simple measure of a deviatory scalar series, the skewness (i.e., the third moment of the series nondimensionalized by the three-halves power of the variance), appeared to consistently predict the sign of the flux during LeadEx. The approach is illustrated in Figure 6. At lead 3, 1-hour time series of deviatory temperature and salinity (linearly detrended) from TIC 2 were used to estimate normalized probability density functions (pdf's); for example, for temperature, the normalized, discrete pdf is the histogram of T'/σ divided by $N\Delta x$, where σ is the sample standard deviation, N is the number of samples, and Δx is the width of the histogram bins. Results were averaged in histogram bins for all 1-hour time series for which covariance heat flux exceeded 5 W m^{-2} (upward). Similar calculations were made for all 1-hour time series for which heat flux was less than -5 W m^{-2} (downward). Average discrete pdf's are shown along with standard normal distributions (zero mean, unit variance) for T' and S'. The discrete distributions are noticeably asymmetric with tails weighted toward positive excursions in

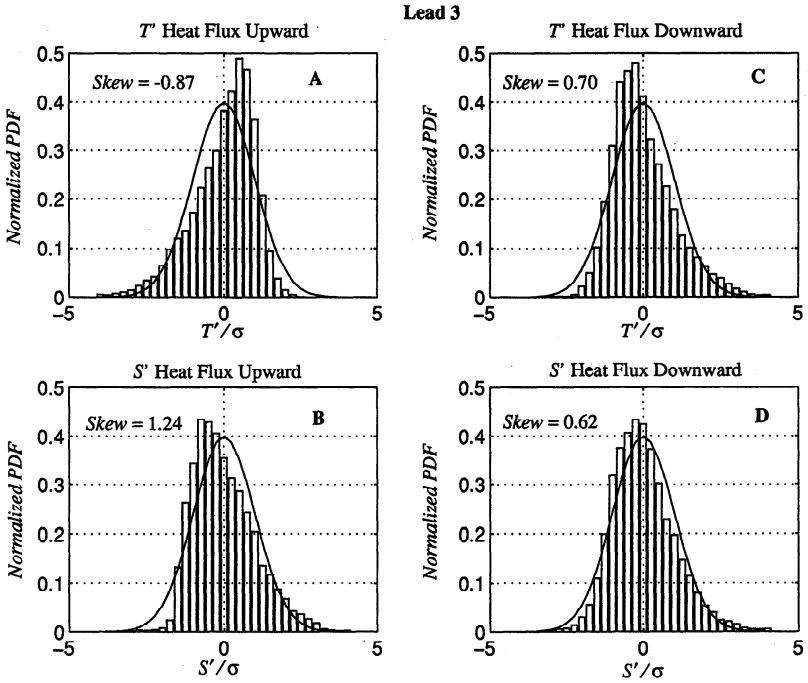

Figure 6. Normalized probability density functions from histograms of T' and S', averaged over 1-hour segments. (a, b) Heat flux upward refers to average of 20 samples for which heat flux exceeded 5 W m^{-2}; (c, d) heat flux downward refers to the average of 9 samples when heat flux was less than -5 W m^{-2}. Data are from turbulence instrument cluster (TIC) 2 at lead 3. Solid curves show the standard normal distribution (mean 0, variance 1).

each case where scalar flux was downward (recall that salinity and buoyancy flux were down regardless of heat flux direction). Mean values of skewness (a measure of the asymmetry of the pdf) calculated for each 1-hour time series are also shown. In general, for each 1-hour realization of the deviatory scalars, skewness was an order of magnitude greater than the expected standard deviation of skewness estimates if the underlying distribution were normal [*Press et al.*, 1988]. For TIC 2, there was perfect anticorrelation between signs of scalar flux and skewness for all samples in which heat flux magnitude exceeded 5 W m^{-2}.

Thorpe et al. [1991] reported similar correspondence between inferred heat flux and the skewness of the time derivative of temperature measured with a thermistor array towed in the upper ocean. For downwind tows (like the ice drift), positive heat flux (convective cooling) was associated with positive skewness and vice versa. I performed a similar analysis by taking numerical time derivatives of the temperature and salinity series and found results compatible with those of *Thorpe et al.* [1991]. However, the time derivative skewness did not appear to be as robust an indicator of flux direction as the straight time series skewness (Table 1). For all clusters and all 1-hour data segments for which vertical heat flux magnitude exceeded 5 W m^{-2} at lead 3, the sign of the skewness of T' predicted flux direction correctly 97% of the time. For downward salinity flux measured with TIC 2, skewness of both salinity and its time derivative were perfect predictors when flux magnitude exceeded 5×10^{-6} psu m s^{-1}.

Results here suggest reexamining the meaning of the turbulent scale velocity in convective boundary layers. At lead 3 the mean value of u_* from the measured Reynolds stress during the time depicted in Figure 5 was 0.63 cm s^{-1}, almost the same as the mean value of convective scale velocity based on the mixing length from the w spectrum ($w_* = (\langle w'b' \rangle \lambda)^{1/3}$), which was 0.65 cm s^{-1}. The alternative convective scale velocity based on mixed layer depth, W_*, was about twice as large, 1.3 cm s^{-1}. Previous results [*McPhee*, 1994; MS] along with the arguments above indicate that the lower value better describes the turbulent scale velocity for lead 3 and hence that the appropriate length scale in (2) is probably much less than the mixed layer depth. J. Morison (personal communication, 1996) has pointed out an interesting interpretation of the convective scale velocity under leads moving at speed U_{ice} with respect to

Table 1. Skewness as a Predictor of Vertical Flux Direction

Variable	Skewness	Skewness Standard Deviation	Score, %	Samples
T'*	−0.83	0.48	97	76
T'†	0.67	0.39	95	41
dT/dt*	0.37	0.51	84	76
dT/dt†	−0.28	0.70	73	41
S'‡	0.94	0.30	100	21
dS/dt‡	−0.28	0.16	100	21

Heat flux up indicates 1-hour samples from all clusters at lead 3 for which the covariance heat flux exceeded 5 W m^{-2}; down is for heat flux less than -5 W m^{-2}. Deviatory salinity is from turbulence instrument cluster (TIC) 2, which was equipped with a microstructure conductivity sensor. Hourly samples were considered if the salinity flux was less than -5×10^{-6} psu m s^{-1}. Buoyancy flux followed salinity flux in all cases. Column labeled "Score" is the percentage of the samples for which the flux direction was correctly predicted by the skewness.

*Heat flux up.

†Heat flux down.

‡Flux down.

the undisturbed ocean; namely, if x is the distance from the upstream (leading) edge, the depth of influence of the convective boundary layer associated with the lead will increase as the ratio $w_* x/U_{ice}$ until it reaches the mixed layer depth. Past the point $X = U_{ice}D/w_*$, the convective boundary layer will be "fully developed." At lead 3, depending on the definition used for convective scale velocity, X was either roughly 550 m (w_*) or 275 m (W_*) in a 1-km-wide lead. In either case it is likely that from our vantage point at the downstream edge the turbulent regime and, for example, the horizontal spacing of the energetic convective cells (about twice the mixed layer depth at lead 3) was fully developed and limited by the mixed layer depth. At lead 4, however, the mixed layer depth was nearly the same as at lead 3, with w_* and W_* values of about 0.5 and 1.1 cm s^{-1}, respectively (section 2). Corresponding values for X are 214 m (w_*) and 98 m (W_*). The lead was ~100 m wide, so in this case the choice of convective velocity scale may be important for interpreting measurements made at the trailing edge. Assuming for the sake of argument that the spacing of the convective cells varies with the depth of influence suggested by Morison, we might expect the cell spacing at lead 4 to be similar to lead 3 if W_* is the proper scale or to be considerably less if w_* is the scale. In fact, the spectrum of Figure 2b is representative of most of the salinity spectra at lead 4, and the horizontal separation scale associated with the spectral peak is of order 20 m, which is only a third of the cell spacing observed at lead 3. So here too the implication is that W_* is an overestimate of the convective scale velocity. Variation of properties across lead 4 is discussed in more detail by *Morison and McPhee* [this issue]. The second example illustrates that w_* is not always uniquely related to W_* since the convective turbulent length scale is not necessarily proportional to the mixed layer depth, defined as the depth where the pycnocline starts.

The hypothesis put forth here is that in a boundary layer flow where the main source of turbulence is destabilizing buoyancy flux (rather than shear driven stress), information needed to assess vertical flux magnitude resides in the wavenumber spectrum of the scalar variable that controls buoyancy. Given limitations imposed both by the short data record and by the difficulty of determining vertical velocity when mean horizontal flow is small, the present results are encouraging but far from definitive. If proved valid, the hypothesis provides a valuable tool for studying convective mixing, which may used in addition to (or in lieu of) conventional microstructure profiling techniques that rely on measuring dissipation rates at very small scales. An obvious application is using autonomous underwater vehicles [*Morison and McPhee*, this issue] for rapid horizontal sampling of temperature and salinity deviation ensembles in the mixed layer when surface stress is small and freezing (or cooling in more temperate climates) is large. The free convection IDM requires only that the spectrum be measured into the inertial subrange, a much less stringent requirement than measuring out to dissipation wavenumbers. It also provides concrete estimates of the length and velocity scales characterizing the turbulent exchange process.

Acknowledgments. The impetus for this work came from discussions with J. Morison on interpretation of autonomous underwater vehicle measurements. Funding was provided by the Office of Naval Research, through contracts N00014-94-C-0023 and N00014-96-C-0032, and the National Science Foundation, through grant OPP 9410848.

References

Edson, J. B., C. W. Fairall, P. G. Mestayer, and S. E. Larsen, A study of the inertial-dissipation method for computing air-sea fluxes, *J. Geophys. Res.*, *96*, 10,689–10,711, 1991.

Gross, T. F., and A. R. M. Nowell, Spectra scaling in a tidal boundary layer, *J. Phys. Oceanogr.*, *15*, 496–508, 1985.

Hinze, J. O., *Turbulence*, 2nd ed., 790 pp., McGraw-Hill, New York, 1975.

LeadEx Group, The LeadEx Experiment, *Eos Trans. AGU*, *74*(35), 393, 396–397, 1993.

McPhee, M. G., On the turbulent mixing length in the oceanic boundary layer, *J. Phys. Oceanogr.*, *24*, 2014–2031, 1994.

McPhee, M. G., and D. G. Martinson, Turbulent mixing under drifting pack ice in the Weddell Sea, *Science*, *263*, 218–221, 1994.

McPhee, M. G., and T. P. Stanton, Turbulence in the statically unstable oceanic boundary layer under Arctic leads, *J. Geophys. Res.*, *101*, 6409–6428, 1996.

Morison, J. H., and M. G. McPhee, Lead convection measured with an autonomous underwater vehicle, *J. Geophys. Res.*, this issue.

Morison, J. H., M. G. McPhee, T. B. Curtin, and C. A. Paulson, The oceanography of winter leads, *J. Geophys. Res.*, *97*, 11,119–11,218, 1992.

Press, W. H., B. P. Flannery, S. A. Teukolsky, and W. T. Vetterling, *Numerical Recipes in C: The Art of Scientific Computing*, 735 pp., Cambridge Univ. Press, New York, 1988.

Shay, T. J., and M. C. Gregg, Convectively driven turbulent mixing in the upper ocean, *J. Phys. Oceanogr.*, *16*, 1777–1798, 1986.

Thorpe, S. A., M. Curé, and M. White, The skewness of temperature derivatives in oceanic boundary layers, *J. Phys. Oceanogr.*, *21*, 428–433, 1991.

M. G. McPhee, McPhee Research Company, 450 Clover Springs Road, Naches, WA 98937. (e-mail: miles@wolfenet.com)

(Received August 15, 1996; revised December 23, 1996; accepted December 30, 1996.)